



ELSEVIER

Available online at www.sciencedirect.com



Electric Power Systems Research 74 (2005) 167–175

ELECTRIC
POWER
SYSTEMS
RESEARCH

www.elsevier.com/locate/epshr

Topology error identification using a two-stage DC state estimator

Lin Xu, Kevin Tomsovic*, Anjan Bose

School of Electrical Engineering and Computer Science, Washington State University, P.O. Box 642752, Pullman, WA 99164-2752, USA

Received 29 September 2004; accepted 22 October 2004

Available online 11 January 2005

Abstract

One of the fundamental tenets in deregulation of the power system is to provide fair and open access to transmission facilities. This requires that market participants, both power brokers and generation companies, have complete and timely information as to the transmission availability. The present system of posting available transmission capacities (ATC) is useful but limited because there is no information to predict how these ATCs will change with changing power transfers. It has been proposed that all traders have access to the real-time data of the full transmission model, i.e., state estimator results from the control centers, but this may be too complex and voluminous to be useful to the traders. Instead, making DC power flow data for real-time conditions may provide enough transmission data for traders to make knowledgeable decisions. In this paper, we show how the results of a DC state estimator can be accurately made available to all concerned.

© 2004 Elsevier B.V. All rights reserved.

Keywords: State estimator; Available transfer capacities; ISO

1. Introduction

The constraint that the transmission grid poses on the free trading of electrical energy is a constant source of frustration to both power brokers and generation companies. The present system of posting available transfer capacities (ATC) on the OASIS system does not provide enough information for the traders to predict under what levels of transaction the system will face congestion. For such full transparency, each participant should be able to determine this availability independently. One way to achieve this is to make available to all participants the state estimator results that are available to the ISO/RTO. Although, this will certainly allow the traders to participate or verify all ISO decisions on transmission constraints, it will also require the traders to have the same level of sophisticated software tools as the ISOs to do so. The investment needed in expertise and software for this level of information exchange may be unfair to the smaller brokers or generation owners.

An alternative suggestion is to provide all participants with DC power flow data for real-time conditions. Given that many ISOs are adopting methods based on distribution factors to make transmission decisions, the DC power flow may be accurate enough for the traders to anticipate transmission constraints and make informed decisions. On the other hand, DC power flow data can be handled with readily available off-the-shelf software or easily integrated into existing trading software. This paper addresses how accurate DC power flow results of real-time conditions can be made available. A DC state estimator is proposed and a method is developed to correct for topology errors. In all state estimation, a topology error, unlike an analog measurement error, can make the state estimator results useless and much research is available for topology error detection and correction for the AC state estimator. We present a novel two-stage DC state estimator that can correct for topology errors.

The traditional full AC state estimator has many technical advantages in the detection and identification of errors. Unfortunately, it suffers from several disadvantages from a trader's viewpoint. First, it requires a large amount of data, all of which may introduce new errors or observability problems and most of which will not be directly relevant to a

* Corresponding author. Tel.: +1 509 335 8260; fax: +1 509 335 3818.

E-mail addresses: linxu@ieee.org (L. Xu), kevin.tomsovic@wsu.edu (K. Tomsovic), bose@eeecs.wsu.edu (A. Bose).

given trade. Second, convergence problems that often arise in practice are an unnecessary complication for the purposes of conducting transactions. Third, many of the market rules that are of concern to a trader are based on a simplified DC power flow, such as in the flowgate model [1], so that the resulting state estimate must be modified to be meaningful for the market.

This paper addresses these problems by beginning with a DC state estimator and adjusting the topology error processing for such a system view. The authors suggest that traders given access to select real-time data could operate such an estimator independently. The primary difficulty is in the inherent errors in the DC model that limit topology error processing. In the proposed approach, state estimation is performed at the bus/branch level. If any errors are detected, the suspect area is expanded into a bus-section/switching-device model. Then, the state estimate is repeated over this expanded model. A new method is proposed that more effectively distinguishes between modeling approximation errors and data errors.

There exists extensive literature that addresses the topology error identification problem. Monticelli and co-workers [2–4] used a physical level model and modeled the zero-impedance branch by its power flow. By assessing this flow, one can tell the status of the zero-impedance branch. However, pinpointing the suspicious area is crucial, otherwise the method suffers computationally. Liu and Wu [5,6] and Clements and Davis [7] both modeled the topology error as a change in the measurement matrix, and subsequently identify the error analytically. Lugtu et al. [8] used residual analysis and empirical judgment to determine the topology error. Abur et al. [9] has proposed a two-stage method similar to our approach. All of the above approaches use full AC state estimation. In the proposed method, the modeling error is estimated in order to compensate for the inherent inaccuracy of the DC method, while maintaining the advantages of robustness and efficiency. Further, these linear computations are more appropriate from a market viewpoint.

2. Background

2.1. DC state estimation

In this section, we first review the classical formulation of the state estimation and a liberalized version of it. A model is introduced that includes the topology errors and model (DC) error. The nonlinear equations relating the measurements z and the state vector x are:

$$z = H(x_{\text{true}}) + \varepsilon \quad (1)$$

where ε is measurement error vector with zero mean and covariance matrix R . With a linear model of the power system (bus angle θ_i as x_{true} , real power injection P_i and line flow P_{ij}

as measurement z), (1) simplifies to:

$$z = Hx_{\text{true}} + \varepsilon \quad (2)$$

where H is the Jacobian matrix. The state estimation problem usually is formulated as a least square problem (WLS) to minimize:

$$J(x) = (z - Hx)^T W(z - Hx) \quad (3)$$

where W is a weighting matrix (inverse of the covariance matrix) and x is the state vector.

2.2. Error modeling

There are three different types of errors in the DC model:

1. Measurement error
2. Model error
3. Topology error

Measurement error: Measurement error can be modeled as a zero mean with non-zero covariance, assuming no gross error exists. *Model error:* Since the linear model is only an approximation to the real system model, another error is added to the linear model:

$$z = Hx_{\text{true}} + \gamma + \varepsilon \quad (4)$$

where γ is the model error vector, i.e., the difference between the accurate model and DC model. It is not a random but a deterministic value that depends on the current state of the system. *Topology error:* If topology errors exist, the model becomes:

$$z = (H + dH)x_{\text{true}} + \gamma + \varepsilon \quad (5)$$

where dH is introduced by the incorrect topology. There are several kinds of topology errors of interest here. *Branch outage and addition:* Incorrect information on the breaker of the line/branch will cause false line outage condition. For example, the false line i - j outage will result in errors on:

- Branch flow measurement error on the row regarding the line measurement.
- Injection measurement error on the row of i and j .

These can be modeled as additional or reduced line flow from the corresponding line or node [6,7]. Assume there is a false status on line i - j , which should be an outage instead of an operation, as illustrated in Fig. 1.

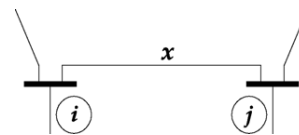


Fig. 1. Line i - j with impedance x .

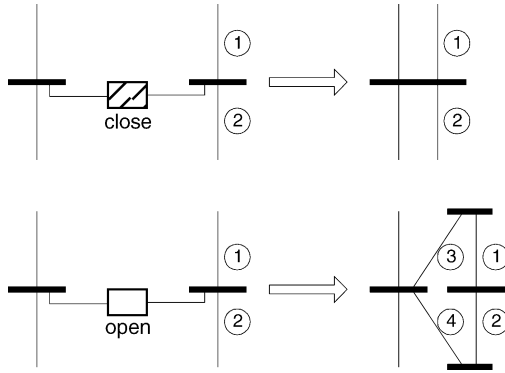


Fig. 2. Modeling bus split as line outage and addition.

For a line flow measurement, the corresponding row of H matrix related to the flow measurement P_{ij} on line i – j has the following change:

$$\left[\dots \quad -\frac{1}{x} \quad \dots \quad \frac{1}{x} \quad \dots \right]$$

For an injection measurement, the corresponding row of the H matrix related to the injection measurement on node i changes by:

$$\left[\dots \quad -\frac{1}{x} \quad \dots \quad \frac{1}{x} \quad \dots \right]$$

and similarly for the row of the H matrix related to the injection measurement on node j .

Bus split: False breaker status can result in a different configuration of the substation. Bus split can be modeled as multiple line outages and additions [5,6]. For example, in Fig. 2, a bus split can be modeled as outages of line 3 and 4 and additions of line 1 and 2.

3. Proposed approach

The approach to topology error identification is using two-stage state estimation. The first stage is using state estimation on bus/branch model, if suspect area detected, this area is converted to detailed bus section/switching device model, then a second stage generalized state estimation is used on the mixed model to identify the topology error. DC state estimation has an advantage over AC here, since the DC estimator can greatly reduce the calculation burden on the mixed model and only moderate accuracy is needed at this stage. The primary concerns are: one, the relative accuracy of the DC state estimation, and two, indices that can pinpoint the error location. In the following section, various methods to improve DC state estimation are presented. Two indices on topology identification are introduced in Section 5. Calculations on test cases reveal that this approach is feasible.

4. DC state estimation solution methods

4.1. Conventional WLS method

The well-known solution to (3) is:

$$\hat{x} = G^{-1} H^T W z \quad (6)$$

where G is gain matrix, and

$$G = H^T W H \quad (7)$$

The residual value for an estimation is defined as:

$$r = z - H \hat{x} \quad (8)$$

Assuming only measurement errors ε are present, simple algebra shows:

$$r = S \varepsilon \quad (9)$$

where

$$S = I - H(H^T W H)^{-1} H^T W \quad (10)$$

The expected values for \hat{x} and r are then unbiased with covariance:

$$\text{cov}(\hat{x}) = G \quad (11)$$

$$\text{cov}(r) = S W^{-1} \quad (12)$$

If model errors are present, (9) becomes:

$$r = S(\varepsilon + \gamma) \quad (13)$$

The expected values for \hat{x} and r are no longer unbiased and become:

$$E(\hat{x}) = x_{\text{true}} + G^{-1} H^T W \gamma \quad (14)$$

$$E(r) = S \gamma \quad (15)$$

4.2. WLS with linear equality constraints

One way to improve the accuracy of conventional WLS DC state estimation is to treat virtual measurements (zero injections) as linear equality constraints. There are several methods to deal with these constraints. A simple approach used here is to simply weight heavily (i.e., assume some small covariance) any virtual measurement.

4.3. Total least squares (TLS) method

Since the DC model is not accurate due to model error, another possible improvement is to correct the matrix H instead of estimating model error. This leads to a class of problems called TLS problems [10–12]. This is described in the following. The objective is to minimize:

$$\|D[E, \varepsilon]T\|_F \quad (16)$$

subject to:

$$(H + E)x = z + \varepsilon \quad (17)$$

where $H, E \in \mathbb{R}^{m \times n}$, $x \in \mathbb{R}^{n \times 1}$, $z, \varepsilon \in \mathbb{R}^{m \times 1}$ and $D \in \mathbb{R}^{m \times m}$, $T \in \mathbb{R}^{(n+1) \times (n+1)}$; E and ε are unknown; and D, T are weighting matrices.

Thus, the model error can be partially eliminated when estimating x . The literature [12] and our calculations reveals that in typical applications, gains of 10–15% in accuracy can be obtained by using TLS instead of standard least squares methods.

The condition for the TLS problem to have a unique solution is that the least singular value of H is larger than the least singular value of $[H, z]$. For typical state estimations, these conditions are satisfied. The common method to solve TLS problem is using singular value decomposition (SVD) (see Appendix A). If $D[H, z]T = U \Sigma V^T$ and U, Σ, V are partitioned (with dimensions shown) as:

$$U = \begin{bmatrix} U_1 & U_2 \\ n & 1 \end{bmatrix}, \Sigma = \begin{bmatrix} \Sigma_{11} & \Sigma_{12} \\ \Sigma_{21} & \Sigma_{22} \end{bmatrix} \begin{matrix} n \\ 1 \end{matrix}, V = \begin{bmatrix} V_{11} & V_{12} \\ V_{21} & V_{22} \end{bmatrix} \begin{matrix} n \\ 1 \end{matrix}$$

then:

$$D[H, z]T = -U_2 \Sigma_2 [V_{12}^T, V_{22}^T] \quad (18)$$

and letting $T_1 = \text{diag}(t_1, \dots, t_n)$ and $T_2 = \text{diag}(t_{n+1})$

$$x = -T_1 V_{12} V_{22}^{-1} T_2^{-1} \quad (19)$$

4.4. Multiple scan methods

The above derivation is based on a single measurement scan. There are several recursive estimation methods based on a dynamic state estimation model that uses a sequence of scans.

4.4.1. Averaging

A natural and simple extension to the common DC state estimation is to average several consecutive results from the state estimator. Suppose n scans is used, in recursive form:

$$\hat{x}_{\text{avg},i} = \frac{\hat{x}_i}{i} + \frac{(i-1)\hat{x}_{\text{avg},i-1}}{i} \quad (20)$$

where \hat{x}_i is the estimation from the i th measurement z_i . $i = 1, \dots, n$ and $\hat{x}_{\text{avg}} = \hat{x}_{\text{avg},n}$. Assuming measurement errors are independent between scans, it can be shown that:

$$E(\hat{x}_{\text{avg}}) = E(\hat{x}_i) \quad (21)$$

and

$$\text{cov}(\hat{x}_{\text{avg}}) = \frac{1}{n} \text{cov}(\hat{x}_i) \quad (22)$$

Thus, the averaging method generally provides a more consistent result, but it does not remove any bias that may arise, as would occur with a modeling error.

Kalman filter [13]: Assuming that the states of the power grid do not change quickly in a short period, the following equations for the power system can be established at snapshot i :

$$x_{i+1} = x_i + q_i \quad (23)$$

$$z_i = Hx_i + v_i \quad (24)$$

where q_i, v_i are Gaussian error vectors, with covariance Q and R , respectively, assuming the covariances are constant in time. The covariance Q is assumed to be small but could be approximated by any number of statistical techniques, including Monte Carlo simulation. Each step of the Kalman filter for the above systems is as follows.

- Start from the prior estimation \hat{x}_i^- and its error covariance matrix P_i^- . Compute the Kalman gain matrix K_i :

$$\begin{array}{c|c} n & \\ \hline 1 & \end{array}$$

$$K_i = P_i^- H_i^T (R + H P_i^- H^T)^{-1} \quad (25)$$

- Update the estimate \hat{x}_i with the i th scan measurement z_i :

$$\hat{x}_i = \hat{x}_i + K_i(z_i - H\hat{x}_i^-) \quad (26)$$

- Compute the error covariance matrix P_i for the updated estimate:

$$P_i = (I - K_i H) P_i^- \quad (27)$$

- Project ahead to predict the new error covariance matrix P_{i+1}^- and new estimation \hat{x}_{i+1}^-

$$P_{i+1}^- = P_i + Q \quad (28)$$

$$\hat{x}_{i+1}^- = \hat{x}_i \quad (29)$$

4.5. Generalized state estimation

Monticelli and co-workers [2–4] introduced the concept of generalized state estimation. Generalized state estimation is performed on a model in which parts of the network can be represented at the physical level, i.e., bus-section/switch-device level. This allows modeling zero-impedance devices and switching devices. It expands the state variables in the conventional state estimation by including load flow through those zero-impedance branches and switch devices. For the linear DC model, the expanded state variable includes real power flows in those zero-impedance devices. Thus, one can judge the status of, say a breaker, by observing the power flow.

5. Topology error detection and identification

Correct detection and identification of the suspect topology error is critical for reducing the calculation of the two-stage estimation. The approach used in this work is using χ^2 -test on $J(x)$ and if it fails (i.e., indicates likely errors), to use the proposed indices to identify the suspect nodes/area. Since the DC model is used here, coexisting modeling errors (4) corrupt the result, in both the χ^2 -test and residual test. This makes correct error detection and identification more difficult. The proposed method tries to estimate and hence, eliminate parts of the modeling error for a more accurate result.

5.1. Error detection

Hypothesis testing and Residual test: Hypothesis testing performs a χ^2 -test on $J(x)$. Since the state estimation is based on the hypothesis that there is no gross error in the measurement, gross errors should result in $J(x)$ and some normalized residuals r_n to be above some threshold. When using the linearized DC state estimation, the inaccuracies in the model itself may cause such a test to fail. Typically, for a large high voltage network, there may be as much as 5% model error. This error corrupts the residual test in several ways:

- One cannot detect topology errors in lightly loaded areas, since the errors may be less than the model error.
- Numerous “false alarms” may occur because the model error is larger than the residual threshold.

When model error is present, $J(x)$ is:

$$\begin{aligned}
 J_{\text{with model error}}(x) &= \sum_{i=1}^m (z_i - \hat{z}_i)^2 / \text{cov}(z_i) \\
 &= \sum_{i=1}^m w_{ii} ((S_i \varepsilon)^2 + 2(S_i \varepsilon)(S_i \gamma) + (S_i \gamma)^2) \\
 &= J_{\text{no model error}}(x) + \sum_{i=1}^m w_{ii} ((S_i \gamma)^2 + 2(S_i \varepsilon)(S_i \gamma)) \quad (30)
 \end{aligned}$$

where m is the number of measurements, S_i the i th row of the projection matrix S , w_{ii} the i th diagonal element of matrix W ; $\hat{z} = H\hat{x}$; γ_i, z_i and \hat{z}_i are the i th component of the γ, z and \hat{z} vector, respectively.

From Eq. (30), one finds that $J(x)$ changes with W, ε and γ . With the existence of the model error γ , the variance of $J(x)$ will increase. Still for a particular case, the model error γ and measurement error ε may cancel each other, leaving less residue. From another point of view, the introduction of model error γ changes the distribution of the $J(x)$. So the threshold of the χ^2 -test must increase significantly, especially

when the covariance of the measurements is small (w_{ii} is large and $|\varepsilon| < |\gamma|$). This increases the difficulty of detecting topology errors with a DC model.

5.2. Estimation of the model error

In Eq. (13), ε is a Gaussian random vector while S and γ are deterministic. One can conceivably estimate γ through r . Unfortunately, S is not of full rank but of rank $m-n$ (where m is the number of measurements and n is the number of states). Thus, γ cannot be estimated completely. This problem belongs to a category called rank-deficient least square problems (see Appendix A).

5.2.1. Method using singular value decomposition (SVD)

One common approach to solving a rank deficiency problem is using SVD. For the model error estimation, rewrite (13) as:

$$r = S\gamma + S\varepsilon \quad (31)$$

The minimal norm solution is:

$$\gamma = V_1 \Sigma_1^{-1} U_1^T r \quad (32)$$

where

$$S = [U_1, U_2] \begin{bmatrix} \Sigma_1 & 0 \\ 0 & 0 \end{bmatrix} [V_1, V_2]^T = U_1 \Sigma_1 V_1^T \quad (33)$$

with U_1, U_2, V_1, V_2 and Σ_1 as given in Appendix A.

Though SVD gives an analytically sound result, it requires more computation than the normal equation. Typically, when $m \gg n$, SVD is about twice the cost of the normal equations and when m is small, SVD is about four times the cost of the normal equations. Since, our goal is to build a simple sound method suitable for traders, by introducing some reasonable simplifications, a faster method is proposed.

5.2.2. A simplified method

Based on some assumptions, portions of the error γ ($m-n$ out of n elements) can be estimated. There are multiple ways to choose the $m-n$ dimension subvector of γ . As [8] illustrates, if sufficient redundancy exists, topology errors tend to affect injection measurements much more than line flow measurements. Selecting those elements of γ corresponding to injections should lead to a better overall result. Assuming, for simplicity, injection measurements are available at every node as well as line flow measurements on every line, the elements in γ corresponding to the injection at each node can be selected as the modeling errors to be estimated.

Doing so is equivalent to assuming that model errors only exist on the node injection measurements with all the modeling errors set to zero. Based on this assumption, (13) becomes:

$$r = S_{\text{node}} \gamma_{\text{node}} + S\varepsilon \quad (34)$$

where S_{node} is an $m \times n$ submatrix of S obtained by deleting all columns that correspond to flow measurements, and γ_{node} is the model error that arises on the node injection measurements. Using similar WLS methods, one obtains:

$$\gamma_{\text{node}} = (S_{\text{node}}^T S_{\text{node}})^{-1} S_{\text{node}}^T r \quad (35)$$

Thus, the modeling error γ is:

$$\gamma = \begin{bmatrix} \gamma_{\text{node}} \\ \gamma_{\text{branch}} \end{bmatrix} = \begin{bmatrix} \gamma_{\text{node}} \\ 0 \\ \vdots \\ 0 \end{bmatrix} \quad (36)$$

5.3. Error identification

If errors are detected, the next step is identification of the specific errors. Correctly locating the suspicious area is the key to reducing the computational effort in the generalized state estimation. If the model error does not change greatly between measurements, one can use the estimated model error for each subsequent scan. In this way, $J(x)$ and r_n indices are representative of measurement errors. To identify topology errors, two indices are proposed in the following.

5.3.1. Node Index

Usually, topology error causes larger errors in the vicinity of those related buses. Thus, simply grouping and averaging the normalized residual r_n by nodes will lead to a better index. The proposed index is built as follows:

Step 1. Initialize arrays Node Index and Node Count to 0.

Step 2. For all r_n

Case 1. $r_n(i)$ is flow measurement on line $i-j$, then add $|r_n(i)|$ to $I(i)$ and Node Index(j), increase both Node Count(i) and Node Count(j) by 1.

Case 2. $r_n(i)$ is an injection measurement node i , then add $|r_n(i)|$ to Node Index(i), increase Node Count(i) by 1.

Step 3. For all nodes

$$\text{Node Index}(i) = \frac{\text{Node Index}(i)}{\text{Node Count}(i)}$$

5.3.2. Topology index

When topology errors are present, the system equation is (5). Using a similar method in estimating modeling error, the residual vector can be written as:

$$r = S(dHx_{\text{true}} + \gamma + \varepsilon) \quad (37)$$

This formulates another estimation problem, if γ has been approximated. Lugtu et al. [8] pointed out that if sufficient

redundancy exists, the topology error would cause the largest residual on the node injection measurement. By using similar method to estimating model error, we can estimate the mismatch $\gamma_{\text{node error}}$ on each node injection.

$$r = S_{\text{node}} \gamma_{\text{node error}} + S\varepsilon \quad (38)$$

The estimated $\gamma_{\text{node error}}$ is used as a topology error index. One expects that large values will appear on the nodes that have topology errors nearby.

6. Test results

The proposed method is evaluated here on the IEEE 30, 39, 57, 118 bus test systems [15].

6.1. Case 1: Comparison of DC and AC state estimation

First, a comparison of DC and AC state estimation is presented. Tables 1–3 show the estimation errors and $J(x)$ for each of the systems. Table 1 shows the result of the WLS method with and without using linear equality constraints. One finds that using linear equality constraints, improves es-

Table 1
WLS method with/without linear equality constraints

| System | With | | Without | | Degrees of freedom |
|--------|-------------|--------|-------------|--------|--------------------|
| | State error | $J(x)$ | State error | $J(x)$ | |
| 30 | 0.0801 | 38.64 | 0.1467 | 33.30 | 41 |
| 39 | 0.1312 | 50.46 | 0.1206 | 45.57 | 46 |
| 57 | 0.0988 | 270.0 | 0.1278 | 78.81 | 80 |
| 118 | 0.1238 | 284.5 | 0.1346 | 200.0 | 186 |

Note: All measurements have 5% Gaussian noise with the error measured as state error = $\sqrt{\sum_i (x_i - \hat{x}_i)^2}$.

Table 2
DC state estimation using TLS

| System | DC | | |
|--------|-------------|--------|-------------------|
| | State error | $J(x)$ | Degree of freedom |
| 30 | 0.0938 | 34.41 | 41 |
| 39 | 0.1103 | 46.28 | 46 |
| 57 | 0.1349 | 98.17 | 80 |
| 118 | 0.1183 | 346.9 | 186 |

Note: All measurements have 5% Gaussian noise with the error measured as state error = $\sqrt{\sum_i (x_i - \hat{x}_i)^2}$.

Table 3
AC state estimation

| System | AC | | |
|--------|-------------|--------|-------------------|
| | State error | $J(x)$ | Degree of freedom |
| 30 | 0.0113 | 8.538 | 164 |
| 39 | 0.0217 | 118.1 | 184 |
| 57 | 0.0236 | 23.46 | 320 |
| 118 | 0.0312 | 113.5 | 744 |

Note: All measurements have 5% Gaussian noise with the error measured as state error = $\sqrt{\sum_i (x_i - \hat{x}_i)^2}$.

Table 4
Estimation with no model error correction

| System | IEEE 30 BUS | | | |
|---------|-------------|--------|-------------------|-----------------|
| | State error | $J(x)$ | Degree of freedom | $\chi^2 > 0.99$ |
| Kalman | 0.021 | 56.82 | 41 | 64.95 |
| Average | 0.021 | 80.12 | 41 | 64.95 |
| DC | 0.0238 | 47.12 | 41 | 64.95 |
| AC | 3.62E-05 | 10.75 | 164 | 209.0 |

Note: All measurements have 5% Gaussian noise with the error measured as state error = $\sqrt{\sum_i (x_i - \hat{x}_i)^2}$.

timization accuracy. This is important, as a typical large system has many buses with zero injection. Table 2 shows the estimation results using TLS. As expected, the results improve slightly in terms of the state error. Next, Table 3 shows the estimation result obtained by using AC state estimation. It is listed here for comparison only. Obviously, it is more accurate than the DC methods. Still, the improvement is not tremendous and the DC method appears sufficiently accurate. These results show that model correction reduces $J(x)$ when no large error is present, thus decreasing the chance of a “false alarm.”

6.2. Case 2: Benefit of model error correction

The result of three different estimation methods, conventional WLS method, averaging and Kalman filter are presented on the system with no measurement and topology errors. Tables 4 and 5 show the estimation errors with and without model error correction, respectively, under typical loading conditions.

6.3. Case 3: Error detection and identification

6.3.1. Single topology error

A test is carried out on the IEEE 57 bus system [15]. In this case, we simulate a false breaker status on line 15–14 (i.e., false branch outage on branch 15–14).

6.3.1.1. No gross measurement error. Here, there are 5% Gaussian errors on each measurement but not gross measurement error. With the degrees of freedom ($m-n$) = 81, a confidence level of 0.95, the threshold for the residual test is 103.01. We find $J(x)$ = 4032, which clearly indicates that errors exist. For identification, the node and topology indices

Table 5
Estimation with model error correction

| System | IEEE 30 BUS | | | |
|---------|-------------|--------|-------------------|-----------------|
| | State error | $J(x)$ | Degree of freedom | $\chi^2 > 0.99$ |
| Kalman | 0.0169 | 37.08 | 41 | 64.95 |
| Average | 0.0238 | 55.09 | 41 | 64.95 |
| DC | 0.0167 | 33.95 | 41 | 64.95 |

Note: All measurements have 5% Gaussian noise with the error measured as state error = $\sqrt{\sum_i (x_i - \hat{x}_i)^2}$.

Table 6
Three indices: Case 3a

| r_n Test | | Node Index | | Topology Index | |
|------------|---------|------------|-------|----------------|--------|
| Meas. | $ r_n $ | Node | Value | Node | Value |
| Inj. 14 | 58.67 | 14 | 42.15 | 15 | 0.718 |
| Ln. 14–13 | 55.47 | 46 | 23.89 | 14 | 0.624 |
| Inj. 46 | 48.78 | 13 | 13.31 | 1 | 0.271 |
| Inj. 47 | 21.84 | 47 | 11.22 | 8 | 0.258 |
| Inj. 15 | 17.22 | 49 | 7.948 | 13 | 0.153 |
| Inj. 13 | 14.54 | 15 | 7.363 | 9 | 0.127 |
| Ln. 14–46 | 12.30 | 51 | 6.073 | 3 | 0.0542 |
| Ln. 47–46 | 10.58 | 50 | 6.030 | 12 | 0.0518 |

Note: Prefixes Inj., Ln. in the Meas. column represent power injection and line flow measurement, respectively. Power values are in p.u.

are used. The errors at the largest eight nodes, ranked in ascending order, are shown in Table 6. For comparison, the r_n index is also listed. From these three indices, one can immediately find that all indices are able to identify the topology error. Among them, the topology index most clearly pinpoints nodes 15 and 14 as the largest. A second step using generalized state estimation shows that the line flow on line 15–14 is 0.65, large enough to indicate that the breaker is closed. The true value of line flow 15–14 is 0.70.

6.3.1.2. With gross measurement error. Besides the 5% Gaussian error, a 70% gross error is included for the measurement on line 13–12. $J(x)$ is 4653, which clearly indicates error. Table 7 shows the three indices in this case. One finds that topology error has more impact on the indices than gross measurement error. And once again, these indices can identify the topology error. Applying generalized state estimation, the estimated value on line 15–14 is 0.634, indicating the incorrect breaker status.

6.3.2. Multiple topology errors

This test is using the IEEE 30 system [15]. Topology errors are introduced for the breaker status on lines 27–30 and 10–20, i.e., false branch outages on branch 27–30 and 10–20. The three indices are shown in Table 8. In this case, the proposed indices especially, the topology index, are better than

Table 7
Three indices: Case 3B

| r_n Test | | Node Index | | Topology Index | |
|------------|---------|------------|-------|----------------|--------|
| Meas. | $ r_n $ | Node | Value | Node | Value |
| Inj.14 | 61.96 | 14 | 43.83 | 15 | 0.696 |
| Ln.14–13 | 57.32 | 46 | 24.93 | 14 | 0.680 |
| Inj. 46 | 50.99 | 13 | 14.49 | 1 | 0.175 |
| Inj. 47 | 19.78 | 47 | 11.76 | 13 | 0.0691 |
| Inj. 15 | 18.67 | 49 | 8.210 | 8 | 0.0656 |
| Inj. 49 | 17.18 | 15 | 8.137 | 12 | 0.0427 |
| Ln. 49–48 | 12.66 | 51 | 6.605 | 26 | 0.0420 |
| Inj.14–46 | 12.22 | 50 | 5.792 | 44 | 0.0280 |

Note: Prefixes Inj., Ln. in the Meas. column represent power injection and line flow measurement, respectively. Power values are in p.u.

Table 8
Three indices: Case 3c

| r_n Test | Node Index | | Topology Index | | |
|------------|------------|-------|----------------|-------|--------|
| | Node | Value | Node | Value | |
| Inj. 20 | 16.00 | 20 | 12.84 | 10 | 0.0983 |
| Ln. 19–20 | 9.687 | 30 | 9.026 | 20 | 0.0917 |
| Inj. 30 | 9.275 | 19 | 7.456 | 27 | 0.0802 |
| Ln. 29–30 | 8.776 | 27 | 4.927 | 30 | 0.0683 |
| Inj. 10 | 8.390 | 29 | 4.850 | 4 | 0.0560 |
| Inj. 19 | 7.258 | 10 | 3.979 | 1 | 0.0480 |
| Inj. 12 | 6.861 | 16 | 3.455 | 2 | 0.0472 |

Note: Prefixes Inj., Ln. in the Meas. column represent power injection and line flow measurement, respectively. Power values are in p.u.

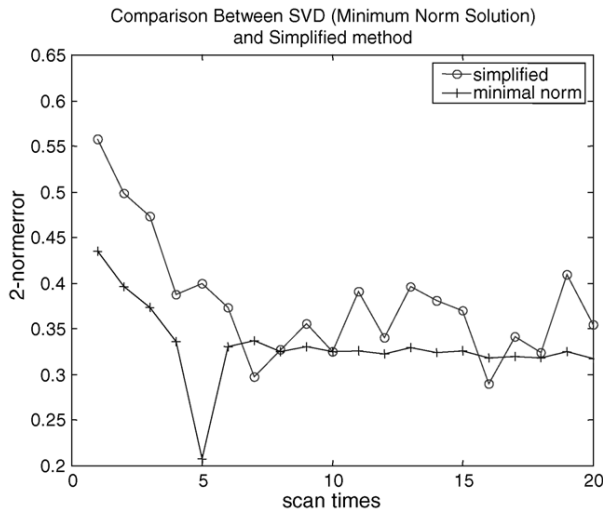


Fig. 3. Performance comparison between SVD and proposed method.

the r_n index, since they provide a clearer view of the errors in the system. This shows that the proposed methods are also valid for identifying multiple topology errors.

6.4. Case 4: Comparison of SVD and the proposed method

A comparison is made based on the difference between the estimated error \hat{e} and the actual model error e , i.e., $\sqrt{\sum_i (e_i - \hat{e}_i)^2}$, over successive scans. As one might expect the SVD achieves more consistence results, but the performance is quite similar. Since the proposed method requires far less computation, it is suggested here as the preferred method as shown in Fig. 3.

7. Discussion and conclusions

A two-stage DC estimation is proposed to detect and identify topology errors. In the first stage, state estimation is performed on the bus/branch level. When errors are detected, the suspicious area is converted to bus-section/switching-device level and the second stage state estimation is performed. Mul-

iple scan DC state estimation methods are introduced. The DC model modeling error is also partly estimated. Results on several IEEE test systems show the validity of the method.

The DC estimator is not proposed here to be a replacement for a full AC estimator, which might be needed by the system operator, but rather as a simplified view of the power system appropriate for certain market participants. An open electricity market has many players with different viewpoints of the system and needs for accuracy. DC state estimation has many advantages and could easily be implemented outside the control center given availability to select measured data and system parameters. Further, the results can be more easily related to typical market rules. The authors suggest that where the proposed estimator begins to break down under the burden of modeling errors, it is also likely that the limits of the trading rules will begin to be reached.

Appendix A

Singular value decomposition and rank-deficient least square problems [10,11,14]

Singular value decomposition (SVD): Any $m \times n$ matrix A with $m \geq n$ can be written as:

$$A = U \Sigma V^T \quad (39)$$

where U is m -by- n and satisfies $U^T U = 1$ and $\Sigma = \text{diag}(\sigma_1, \dots, \sigma_n)$ with $\sigma_1 \geq \dots \geq \sigma_n \geq 0$. The columns, u_1, \dots, u_n , of U are called left singular vectors. The columns v_1, \dots, v_n , of V are called right singular vectors. The $\sigma_1, \dots, \sigma_n$ are called singular values.

Rank-deficient least square problems (RDLSP): When matrix A is rank deficient or “close” to rank deficient, the least square problems to minimize $\|Ax - b\|_2$ become the so called RDLSP SVD is one of the most commonly used methods to solve this kind of problems. For the rank deficiency least square problem, let A be an m -by- n with $m \geq n$ and $\text{rank}(A) = r < n$. There is an $n-r$ dimensional set of vectors x that minimize $\|Ax - b\|_2$. When A is singular, the SVD of A is:

$$A = [U_1, U_2] \begin{bmatrix} \Sigma_1 & 0 \\ 0 & 0 \end{bmatrix} [V_1, V_2]^T = U_1 \Sigma_1 V_1^T \quad (40)$$

where Σ_1 is $r \times r$ and nonsingular, and U_1 and V_1 have r columns. Let $\sigma = \sigma_{\min}(\Sigma_1)$, the smallest nonzero singular value of A . Then the solution x that minimizes $\|Ax - b\|_2$ can be characterized by:

(1) All solutions x can be written as:

$$x = V_1 \Sigma_1^{-1} U_1^T b + V_2 z \quad (41)$$

where z is an arbitrary vector.

(2) The solution x has a unique minimum norm $\|x\|_2$ precisely when $z = 0$, in which case:

$$x = V_1 \Sigma_1^{-1} U_1^T b \quad (42)$$

and

$$\frac{\|x\|_2}{\sigma} \leq \frac{\|b\|_2}{\sigma} \quad (43)$$

Thus, among the $n-r$ dimensional set of solutions, the minimal norm solution (42) for RDSLP exists and is unique.

References

- [1] H. Chao, S. Peck, A market mechanism for electric power transmission, *J. Regul. Econ.* 10 (1) (1996) 25–59.
- [2] A. Monticelli, A. Garcia, Modeling zero-impedance branches in power system state estimation, *IEEE Trans. Power Syst.* 6 (4) (1991) 1561–1570.
- [3] A. Monticelli, *State Estimation in Electric Power Systems, A Generalized Approach*, Kluwer Academic Publishers, 1999.
- [4] O. Alsac, N. Vempati, B. Scott, A. Monticelli, Generalized state estimation, *IEEE Trans. Power Syst.* 13 (3) (1998) 1069–1075.
- [5] F.F. Wu, W.E. Liu, Detection of topology errors by state estimation, *IEEE Trans. Power Syst.* 4 (1) (1989) 176–183.
- [6] W.E. Liu, F.F. Wu, S.M. Lun, Estimation of parameter errors from measurement residuals in state estimation, *IEEE Trans. Power Syst.* 7 (1) (1992) 81–89.
- [7] K.A. Clements, P.W. Davis, Detection and identification of topology errors in electric power systems, *IEEE Trans. Power Syst.* 3 (4) (1988) 1748–1753.
- [8] R.L. Lugtu, D.F. Hackett, K.C. Liu, D.D. Might, Power system state estimation: detection of topology errors, *IEEE Trans. Power Syst.* PAS-99 (6) (1980) 2406–2412.
- [9] A. Abur, H. Kim, M.K. Celik, Identifying the unknown circuit breaker statuses in power networks, *IEEE Trans. Power Syst.* 10 (4) (1995) 2029–2037.
- [10] A. Björck, *Numerical Methods for Linear Squares Problem*, SIAM, Philadelphia, PA, 1996.
- [11] Gene H. Golub, Charles F. Van Loan, *Matrix Computation*, second ed., The Johns Hopkins University Press, 1989.
- [12] S. Van Huffel, J. Vandewalle, *The Total Least Squares Problem: Computational Aspects and Analysis*. Vol. 9 of *Frontiers in Applied Mathematics*, SIAM, Philadelphia, 1991.
- [13] R.G. Brown, Y.C. Hwang Patrick, *Introduction to Random Signals and Applied Kalman Filtering*, John Wiley & Sons, Inc., 1992.
- [14] J.W. Demmel, *Applied Numerical Linear Analysis*, SIAM, Philadelphia, PA, 1997.
- [15] Power Systems Test Case Archive, Department of Electrical Engineering, University of Washington, available: <http://www.ee.washington.edu/research/pstca/> (online).

Lin Xu received the B.S. and M.S. from Southeast University, Nanjing, China, in 1992 and 1995, respectively, all in Electrical Engineering. He is currently pursuing a Ph.D. degree in Electrical Engineering at Washington State University, Pullman, Washington.

Kevin Tomsovic received the B.S. from Michigan Tech. University, Houghton, in 1982, and the M.S. and Ph.D. degrees from University of Washington, Seattle, in 1984 and 1987, respectively, all in Electrical Engineering. He is currently a Professor at Washington State University. Visiting university positions have included Boston University, National Cheng Kung University, National Sun Yat-Sen University and the Royal Institute of Technology in Stockholm. He held the Advanced Technology for Electrical Energy Chair at Kumamoto University in Japan from 1999–2000.

Anjan Bose (M'68, SM'77, F'89) received his Btech. (Hons.) from the Indian Institute of Technology, Kharagpur in 1967, M.S. from the University of California, Berkeley in 1968, and Ph.D. from Iowa State University in 1974. He has worked for the Consolidated Edison Co. of New York (1968–1970), the IBM Scientific Center, Palo Alto (1974–1975), Clarkson University (1975–1976), Control Data Corporation (1976–1981) and Arizona State University (1981–1993). At present, he is the Distinguished Professor in Power Engineering and Dean of the College of Engineering and Architecture at Washington State University.